Sugar-Peptidic Bond Interactions: Spectroscopic Characterization of a Model System

Ander Camiruaga[†,a)], Imanol Usabiaga[†,a)], Aran Insausti, Iker León*[,†,‡], and José A. Fernández*[,†]

† Dpto. de Química Física, Facultad de Ciencia y Tecnología, Universidad del País Vasco-UPV/EHU, Bº Sarriena s/n, Leioa 48940, Spain.

‡ Grupo de Espectroscopía Molecular (GEM), Edificio Quifima, Laboratorios de Espectroscopia y Bioespectroscopia, Unidad Asociada CSIC, Parque Científico UVa, Universidad de Valladolid, 47011 Valladolid, Spain

*E-mail: iker.leon@ehu.es and josea.fernandez@ehu.es

a) A. Camiruaga and I. Usabiaga contributed equally to this work.

ABSTRACT. Sugars are small carbohydrates which perform numerous roles in living organisms such as storage of energy or as structural components. Modifications of specific sites within the glycan chain can modulate a carbohydrate's overall biological function as it happens with nucleic acids and proteins. Hence, identifying discrete carbohydrate modifications and

understanding their biological effects is essential. A study of such processes requires of a deep knowledge of the interaction mechanism at molecular level. Here, we use a combination of laser spectroscopy in jets and quantum mechanical calculations to characterize the interaction between phenyl-β-D-glucopyranoside and N-methylacetamide as a model to understand the interaction between a sugar and a peptide. The most stable structure of the molecular aggregate shows that the main interaction between the peptide fragment and the sugar proceeds via a C=O•••H-O2 hydrogen bond. A second conformer was also found, in which the peptide establishes an C=O•••H-O6 hydrogen bond with the hydroxymethyl substituent of the sugar unit. All the conformers present an additional interaction point with the aromatic ring. This particular preference of the peptide for the hydroxyl close to the aromatic ring could explain why glycogenin uses tyrosine in order convert glucose to glycogen by exposing the O4H hydroxyl group for the other glucoses for the polymerization to take place.

I. INTRODUCTION

Carbohydrates, nucleic acids and proteins are the three major biopolymers that mediate biological processes in living organisms.[1] Sugars are small carbohydrates which perform numerous roles in cells and tissues.[2] For example, polysaccharides serve for the storage of energy and energy management and also play a key role as structural components. Furthermore, saccharides and their derivatives include many other important biomolecules that play key roles in immunity, fertilization, and signaling.[3-7] As an example of their structural importance ribose and deoxyribose are fundamental as backbones of the genetic molecule RNA and DNA respectively. They are also found in glycoproteins that contain oligosaccharide chains (glycans) attached to polypeptide side-chains. The glycans, polysaccharides attached to proteins and lipids, are usually found in the extra-cellular medium, where they act as a cellular I.D.. The cells of the immune system have specialized receptors to probe such glycans and to classify the cells as friends or foes.[3,4] How the polysaccharide accommodates in the receptor decides if an immune response is elicited or not.[5,6] The receptors are designed in such a way that they are able to detect not only modifications in the sequence and nature of the component sugar units, but also in their ramifications and the kind of sugar-sugar bonds: α/β 1-2, 1-3, 1-4… etc.[8,9] A change in the orientation of a single hydroxyl group in a single unit of a long glycan is sometimes enough to change the affinity of the receptor for the glycan, like for example in the case of the blood groups.[7] Finally, sugars are also critical biological markers that modulate the properties of proteins.

These structural functions and modulations of the properties of proteins are guided by the intermolecular interactions between sugar units and other biomolecules. Understanding such processes requires, therefore, of a deep knowledge of the interaction mechanism at molecular level. Very few studies have explored already the sugar-peptide interaction, due mainly to the difficulty that such spectroscopic studies pose: complex laser desorption systems are required to move sugars into gas phase and still a low S/N ratio is usually obtained. Furthermore, the sugar molecules present several hydroxyl groups that congest the IR spectrum, making difficult the assignment unless it is guided by heavy ab initio or DFT calculations. To the best of our knowledge, only

glucose-tyrosine has been explored previously.[10,11] In this work, we chose phenyl-β-D-glucopyranoside (β-PhGlc) and explored its interactions with N-methylacetamide (mAct) using mass-resolved laser spectroscopy in jets. Supersonic expansions create a suitable environment for this purpose: the cold, controlled environment in the expansion allows probing complexes, isolated from any external interaction that may perturb them and facilitates using mass-resolved excitation spectroscopy (MRES) to fully characterize the non-covalent interactions between the interacting molecules. In fact, this technique has already been successfully applied to the study of other systems of biological relevance like amino acids[13-15], peptides,[15-18] neurotransmitters,[19-25], anaesthetics,[26,27] several mono-, di- and poly-saccharides[11,28-33] or even micelles.[34-36]

β-PhGlc was chosen because it has a chromophore, which allows us to perform electronic spectroscopy, and in order to emulate one of the ramifications of an oligosaccharide chain. For example, glycogenin is an important enzyme involved in converting glucose to glycogen which acts as a primer by polymerizing the first few glucose molecules.[37] Polimerization starts with the attachment of the first glucose unit to a tyrosine in the active centre of the enzyme and proceeds with the addition of more sugar units in a head-to-tail manner. On the other hand, mAct was selected as a model of the peptidic bond as it has an amide bond, similar to the essential bond between amino acids in proteins. This is also an important interaction point for hydrogen bonds. Additionally, acetamide is one of the simplest amides which has been detected near the center of the Milky Way.[12] If organic molecules that led to life were initially formed in space and latter integrated on Earth, then complex proteins/peptides, sugars or a combination of both (such as glycans) are an evolution from their simplest units: aminoacids and carbohydrate monomers. Finally, to understand the aggregates, our work is supported with quantum mechanical calculations. The results show that the preferred interaction of the peptide fragment takes place either with the hydroxymethyl moiety forming a C=O•••H-O6 hydrogen bond or with the opposite carbon through a C=O•••H-O2 interaction. The latter results in formation of the most stable specie. The N-H group of the peptide fragment serves as an additional stabilization point and, in this case, interacts with the aromatic ring in the sugar. These results could indicate why nature has selected

glycogenin, and more specifically a tyrosine residue as the docking point of the sugar unit, to convert glucose to glycogen. In a medium where aminoacids are abundant, their preference for the O2H and O6H positions adjacent to the aromatic ring of the sugar hides these hydroxyls leaving only the O4H moiety exposed. Therefore, the probability that a second glucose binds to this position is increased favoring the formation of the glucogen polymerization.

II. EXPERIMENTAL AND THEORETICAL METHODS

A. Experimental methods

The experimental system was described in detail in ref 11 and consists of a modified time of flight mass spectrometer equipped with a laser desorption/ionization (LDI) source attached to a pulsed valve (Series 9, General Valve Inc.), a Nd/YAG-pumped dye laser (Fine Adjustment Pulsare Pro-S), an OPO system (LaserVision) to generate light in the IR region and electronics for synchronization and data collection and handling.

The preparation of the sample was done using a similar procedure to that explained in ref 11 and herein. On the other hand, while β-phenyl-D-glucopyranoside is a solid at room temperature, n-methyacetamide is a viscous solid (melting point 26 ºC). Therefore, the incorporation of N-methylacetamide to the sugar was not easy and a different approach was necessary in order to form the desired molecular aggregates. The procedure is described in detail in Scheme S01 in the supplementary material. As a summary, a drop of liquid glue was deposited on the surface of the cylindrical sample holder allowing us to cover the surface of the holder with a thin layer of active carbon. A homogeneous mixture of carbon nanotubes and β-phenyl-D-glucopyranoside was deposited on the surface of the sample holder once it was dry. Finally, the N-methylacetamide was deposited on top of the sugar/nanotubes sample.

For the REMPI experiments the desorption laser was fired ~ 207 μs after the valve opening, so the sample was picked by the jet. Approximately 200 μs later the UV laser was scanned while the final population of molecules at a given mass channel was recorded. For the IR experiments

similarly the desorption laser was fired ~ 207 μs after the valve opening, so the sample was picked by the jet. Approximately 200 μs later the depopulation IR was fired and the final population of molecules was probed by a UV laser fired 50 ns later. A webcam inside the vacuum chamber allowed us to optimize the alignment of the ablation laser and to monitor the sample at any moment, enhancing the overall performance of the experimental set up.

B. Theoretical methods

A critical aspect of this study was to ensure that the conformational landscape was thoroughly explored, as small, experimentally non-significant changes in the relative orientation of some chemical groups may result in shifts in the IR bands that may derive in incorrect assignments of the experimental spectra. Therefore, to ensure that no important structures were left out, the same computational procedure already tested successfully for similar systems was used.[11,34-36] It consists of three stages. First, an automated exploration of the intermolecular potential energy surface was carried out using fast molecular mechanics methods (MMFFs) and two search algorithms: the "Large scales Low Mode" (which uses frequency modes to create new structures) and a Monte Carlo-based search, as implemented in Macromodel (www.schrodinger.com). In a second stage, the structures were inspected using chemical intuition, looking for alternatives which implicate small rotations or relative positions of functional groups. In this way, a large number of structures were obtained, some of them differing in subtle changes that posed no chemical meaning. Therefore, to compact them into a more manageable number without losing information, they were passed to a clustering algorithm that grouped them into families. Representative structures of each family were then chosen to be subjected to full optimization at the M06-2x/6-311++G(d,p) calculation level as implemented in Gaussian 09,[38] which has proven to yield accurate results for similar systems. A normal mode analysis highlighted the validity of the optimized structures as true minima and allowed us to compute the zero point energy (ZPE). Thus, the energy values given in this work include the ZPE correction. The basis set superposition error was also estimated using the counterpoise procedure of Boys and Bernard.[39]

Finally, the entropy and the Gibbs free energy was calculated for each optimized structure in the 0-700 K interval using the output from the Gaussian calculations and the tools supplied by the NIST (http://www.nist.gov/mml/csd/informatics_research/thermochemistry_script.cfm). A detailed explanation of the procedure can be found in ref 11.

III. RESULTS

A. Exploration of mAct•β-PhGlc potential energy surface

Scheme 1 shows the structures of the mAct and β-PhGlc monomers. The former presents an amide group with two potential interaction points to stablish hydrogen bonds, while the sugar has several hydroxyl groups, two ether groups and an aromatic ring. All the carbons and oxygens in β-PhGlc are labeled in scheme 1 for an easier comparison along this work. Due to the sugar's flexibility, the number of possible isomers of the β-PhGlc•mAct complex is large. In fact, β-Ph monomer presents at least three stable isomers in supersonic expansions, based on the orientation of the hydroxymethyl group.[10] All three structures present a network of cooperative hydrogen bond interactions, although the strength of such contacts is reduced by steric hindrance.

Figure 1 shows the six most stable structures of the complex found in the first 5 kJ/mol relative to the global minimum, calculated at M06-2x/6-311++G(d,p). The rest of structures studied in this work can be found in the supplementary material. Conformer 1, the global minimum, presents a structure stabilized by a hydrogen bond between the sugar's O2-H and the oxygen in the C=O group of mAct, and it is further stabilized by dispersive forces between the N-H group of mAct and the aromatic ring of the sugar. A close view to the structure shows that there is an important extra stabilization resulting from the interaction between the C-H of mAct with the O1 and O2 lone pairs. Also noticeable is the fact that all the hydroxyl groups in the sugar are pointing to the same direction resulting in a cooperative network, as in the isolated sugar.

Conformers 2, 3 and 6 are very similar. The main difference between the global minimum and the second most stable isomer is actually the pointing direction of the O6-H hydroxymethyl

group, and therefore both structures may be connected by a small potential energy barrier. The difference in stability between the two most stable structures highlights the extra stability gained by the cooperative effect. Conformers 3 and 6 are very similar to conformer 2 differing only in a small variation in the relative position of the molecules. In the former, the methyl group of mAct interacts with the aromatic ring of the sugar instead of the amide group; in the later, the mAct is slightly rotated towards the sugar and, despite having an even more directional C=O•••H-O hydrogen bond, there is some destabilization between the hydrogens of the methyl in mAct and those of the hydroxyls in the sugar. Consequently, no significant barriers are expected for isomerization of conformers 3 and 6 into conformer 2.

The rest of the structures adopt different configurations giving a collection of interactions. For example, the fourth most stable isomer adopts a configuration very similar to the global minimum (note also the cooperative effect between the hydroxyl groups in the sugar) but the oxygen in mAct acts as a proton acceptor of the hydroxymethyl O6-H in the sugar instead of the O2-H group. Thus, interacting with the hydroxyl in the second carbon of the sugar gives the cluster an extra stabilization of almost 4 kJ/mol. Finally, conformer 5 is an insertion structure in which the oxygen of the amide group inserts between sugar's oxygens 3 and 4, strongly perturbing the cooperative hydrogen bond network. At the same time, the hydrogens in the peptide's methyl group have some interaction with O3 and O4 lone pair electrons. The first global observation is that the peptide presents always an interaction involving the ketone, making it the key interacting point.

B. Excited state

The complicated landscape of this cluster very likely presents several low-barrier pathways connecting some of the conformers. Therefore, despite that all six structures in Figure 1 could be present in the expansion, the final number of surviving species is probably smaller.

Figure 2 collects the REMPI (resonance enhanced multiphoton ionization) spectra of phenol, β-PhGlc and mAct•β-PhGlc. The mAct monomer cannot be detected using this technique because it lacks a chromophore. On the other hand, β-PhGlc shows a well-defined vibrational structure. The spectrum is in good agreement with the results published by Talbot et al.[10] and reinvestigated by our group.[11]

The REMPI spectrum of the cluster is significantly different from that of the monomer. The 0-0 transition is red shifted by approximately 500 cm^{-1} and it consists of a broad absorption in the 36250 – 37000 cm^{-1} region, with a maximum at c.a. 36575 cm^{-1}. There are two sharp depletions at 36349 cm^{-1} and 36824 cm^{-1} which are due to the presence of phenol in the expansion, also shown in Figure 2 for comparison.[40,41] Phenol is a byproduct of photodissociation of β-PhGlc during the laser desorption. There are a few features which appear as weak peaks over the broad absorption at 36411, 36501 and 36641 cm^{-1}. These bands could be due to vibronic activity or to the presence of several conformers. Unfortunately, due to the low S/N ratio, attempts to record a *hole burning* trace to determine the number of conformers contributing to the REMPI spectrum were not successful. To further explore the REMPI spectrum in a search for additional species, several regions were proved using IR/UV double resonance (see below).

C. Ground state vibrational modes in the 2800-3800 cm^{-1} region.

Despite the fact that the cluster does not present a discrete REMPI spectrum we were still able to record the mass-resolved IR spectrum of the complex, using the technique of IR/UV double resonance, as shown in Figure 3. The IR spectrum of the cluster shows at least two bands in the blue-end of the spectrum, at 3612 and 3630 cm^{-1}. These peaks are due to the stretch vibrations of the OH groups of the sugar that are not involved in any strong interaction. There is another narrow band at 3490 cm^{-1} built on top of a broad absorption that goes from 3250 to 3450 cm^{-1} and with its maximum at 3325 cm^{-1}. Finally, there are several discrete features in the 2800 - 3100 cm^{-1} region, due to the C-H stretching modes.

Comparison between experimental and simulated IR spectra of the computed structures is not straightforward. First, no single conformer alone is able to reproduce the experimental trace and hence at least, two isomers must be contributing to the spectrum. For example, conformer 1 accurately reproduces most of the experimental IR spectrum: the almost unperturbed OH stretching modes should give three peaks; two of them are predicted to have the same frequency and the third one having a slightly higher frequency. The N-H•••π interaction is predicted to give almost no intensity at about 3450 cm^{-1}; finally, this conformer should present a strong hydrogen bond between the O2-H•••O=C groups and hence the O2H stretching mode is predicted to appear red-shifted close to 3350 cm^{-1}. In addition, formation of such strong hydrogen bond induces a strong anharmonicity, transforming the vibronic transition into the broad absorption centered at 3350 cm^{-1}. Still the theoretical IR spectrum of the global minimum fails in reproducing the discrete peak at c.a. 3490 cm^{-1} and part of the broad absorption around 3400-3450 cm^{-1}. Conformers 2 and 3 or even 6, should give a similar IR spectrum, and thus none of them are able to explain the peak at c.a. 3490 cm^{-1}. On the other hand, the simulated spectrum of conformer 4 presents a strong peak at 3490 cm^{-1}, accurately matching the experimental one, pointing to the presence of this conformer in the experiment. Conversely, this conformer alone is not able to reproduce the experimental IR trace, as it fails in reproducing the broad absorption at 3350 cm^{-1}. The spectrum of conformer 5 also shows a peak close to 3490 cm^{-1} but it also predicts a feature at 3580 cm^{-1} that is not observed experimentally so it can be safely ruled out. Hence, the experimental IR trace must be the sum of at least conformers 1 and 4.

IV. DISCUSSION

A. Types of interactions and influence of the entropy

The studies in refs 10 and 11 showed that β-PhGlc presents three conformational isomers, as identified in the REMPI spectrum of the monomer shown in Figure 2, with 0_0^0 transitions at 36868, 36880 and 36903 cm^{-1}. The different conformers correspond to different orientations of the hydroxymethyl moiety connected to carbon 5. Accordingly, several of the conformers calculated for mAct•β-PhGlc and shown in Figure 1 also differ in the orientation of this group: for example, the main difference between conformers 1 and 2 is the orientation of this group where the O6H hydroxyl moiety is in the same basal plane of the sugar, while conformer 5 is a completely different structure with the O6H group out of this plane.

Before making any ground assignment, it is important to take into account the influence of the entropy. In order to predict the stability of a system at temperatures different of the 0 K, as it is the case in the supersonic beam, a thermal energy correction must be added to the total energy, including the effects of translation, rotation and vibration at the corresponding temperature and pressure. Figure 4 shows the relative change in Gibbs Free Energy (ΔG) in the interval of temperatures from the desorption process to the final temperature in the beam. The red bar indicates the temperature at which most of the organic compounds decompose, while the blue bar indicates the temperature of decomposition of pyranose. The dashed box indicates the range of temperatures at which ΔG becomes positive and therefore, the cluster is no longer stable. From an energetic point of view, the six conformers shown in Figure 1 could be formed and detected in the experiment. There are three main observations when the ΔG is taken into account: first, as temperature drops, there is a change of stability between conformers 1 and 2 and at low temperatures conformer 2 is the global minimum. Interestingly, at the temperatures of the supersonic expansion both isomers are almost isoenergetic and thus, both conformers may be present, depending on the height of the potential energy barrier for interconversion; second, conformers 3, 4 and 6 maintain their relative stability; third, stability of conformer 5 experiences the largest dependence on the entropic component in the temperature range of the expansion and therefore it becomes relatively higher in energy as temperature drops, becoming the least stable of the six conformers, almost at 7 kJ/mol with respect to the global minimum, and thus it is not

expected to be found in the expansion or its population should be negligible. Accordingly, the experimental IR spectrum presented in Figure 3 showed no peak at 3580 cm^{-1}, characteristic of conformer 5, and hence this conformer is not detected.

The isomerization barrier of the hydroxymethyl group in β-PhGlc is high enough to detect both species[10]. On the other hand, formation of the complex could result in a lower isomerization barrier. Unfortunately, the difference in the predicted IR spectrum of conformers 1 and 2 is within the calculation error and thus, we cannot distinguish between them. Conformers 3 and 6 are very similar to conformer 2 and, as explained in the results section, they only differ in a small variation of the relative position between mAct and the sugar so it is very likely that these conformers relax into conformer 2 during the initial instants of the expansion. Finally, conformer 4 is found at a relative energy of 4 kJ/mol and hence it is also possible to find it experimentally. This isomer is structurally different from conformers 1, 2 and as it interacts with the aromatic ring and the O6-H hydroxyl group instead of the O2H group, one would expect high energy barriers in the pathway connecting conformer 4 with conformer 2. In agreement, it is the only conformer which is able to explain the sharp peak at 3500 cm^{-1} in the experimental IR spectrum shown in Figure 3 and thus, all the evidences point to the detection of this specie. Therefore, we assign the experimental spectrum to a mix between conformers 1, (2) and 4. A summary of the detected species is nicely illustrated in Figure 5.

B. Conformational preferences

The assignment proposed above would explain the complexity of the REMPI spectrum shown in Figure 2. Furthermore, conformers 1 and 2 can interconvert by the rotation of the methyl group reinforcing the assignment, as this type of clusters are known to have a very active spectrum in the excited state.

Conformers 1 and 2 are almost isoenergetic and are stabilized by a C=O•••H-O2 hydrogen bond, differing only in the orientation of the O6H group and hence they have the same cluster's binding sites. It is interesting how the relative stability between these two conformers switches at

a temperature of about 120 K, highlighting the importance of taking into account the entropy of the system. The other observed conformer, conformer 4 and found at 3.9 kJ/mol, shows the peptide interacting with the hydroxymethyl group forming a C=O•••H-O6 hydrogen bond. An additional stabilization point of the detected species is via the N-H group and the phenolic aromatic ring. These results could indicate why nature has selected glycogenin, and more specifically tyrosine residue, in order to convert glucose to glycogen. Most of the peptides consist of amides, and hence amines and ketones, which are not able to establish strong hydrogen bonds. As these results show, the interaction between a sugar unit and the peptide goes preferentially through interaction with the C=O group, almost ignoring the nitrogen atom. The preferred conformation presents also interaction with the aromatic ring through dispersive forces and therefore, the peptide finds the aromatic ring of the tyrosine an interacting point as energetically favorable as the hydroxyl groups of the sugar. This preference of the aminoacids to interact either with the O2H or O6H hydroxyl groups of the sugar and the aromatic ring at the same time gives extra stabilization to the sugar•aminoacid pair exposing the O4H for the other glucoses to bind. This could favor the formation of the glucogen polymerization in a medium where aminoacids are abundant. Comparison with interaction of phenol,[11] shows that similar structures were found, although in that case the hydroxymethyl group was by all means the preferred interaction site.

V. CONCLUSIONS

We use a combination of mass-resolved laser spectroscopy in supersonic expansions and quantum mechanical calculations to model the interaction between a sugar and a peptide. More precisely, the interaction between phenyl-β-D-glucopyranose and N-methylacetamide system was studied. At least two isomers were found formed by a hydrogen bond between the peptide and the sugar's hydroxyl groups. The most stable structure was stabilized by a C=O•••H-O2 hydrogen bond, while in a second conformer, found at 3.9 kJ/mol, the peptide interacted with the methylhydroxy group forming a C=O•••H-O6 hydrogen bond. Both isomers have an additional stabilization point via the N-H group and the phenolic aromatic ring. This particular preference of

the peptide for the hydroxyls close to the aromatic ring could explain why glycogenin uses tyrosine in order convert glucose to glycogen by exposing the O4H hydroxyl for the other glucoses as peptides could find a more entropically favorable environment by interacting with the hydroxyl groups and the aromatic ring. The results were interpreted though the comparison between the experimental results and the theoretical calculations by taken into account the relative energy and the Gibbs free energy. Other isomers based on the global minimum may also be present and connected through low isomerization barriers, as these isomers are reached either though the rotation of the hydroxymethyl group, as in the sugar monomer, or through a rigid rotation of the peptide with the same contact points.

SUPPLEMENTARY MATERIAL

See supplementary material for a complete set of all the structures, energetics and IR spectra.

ACKNOWLEDGMENT.

The research leading to these results has received funding from the Spanish MINECO (CTQ-2015-68148), FEDER. I. U. thanks the Basque Government for a pre-doctoral fellowship; I.L. thanks the MINECO for a Juan de la Cierva postdoctoral fellowship. Computational and laser resources from the SGI/IZO-SGIker network were used for this work.

References

1. H. A. Lehninger, D. Nelson and M. Cox, Lehninger Principles of Biochemistry, W. H. Freeman, 2008.

2. D. Solís, N. V. Bovin, A. P. Davis, J. Jiménez-Barbero, A. Romero, R. Roy, K. Smetana Jr., and H. Gabius, Biochimica et Biophysica Acta (BBA) - General Subjects, http://dx.doi.org/10.1016/j.bbagen.2014.03.016).

3. H. Ghazarian, B. Idoni, and S. B. Oppenheimer, Acta Histochem. **113**, 236-247 (2011).

4. E. C. Stanca-Kaposta, D. P. Gamblin, E. J. Cocinero, J. Frey, R. T. Kroemer, A. J. Fairbanks, B. G. Davis, and J. P. Simons, J. Am. Chem. Soc. 130, 10691-10696 (2008)6. R. Pal, L. M. Wang, W. Huang, L. S. Wang, and X. C. Zeng, J. Am. Chem. Soc. **131**, 3396-3404 (2009).

5. H. Gabius, S. André, J. Jiménez-Barbero, A. Romero, and D. Solís, Trends Biochem. Sci. **36**, 298-313 (2011).

6. S. Hakomori, and Y. Igarashi, J. Biochem. **118**, 1091-1103 (1995).

7. B. Fiege, C. Rademacher, J. Cartmell, P. I. Kitov, F. Parra, and T. Peters, Angewandte Chemie International Edition, 10.1002/anie.201105719.

8. M. Fernández-Alonso del Carmen, F. J. Cañada, J. Jiménez-Barbero, and G. Cuevas, J. Am. Chem. Soc. **127**, 7379-7386 (2005).

9. T. B. Grindley, in , ed. ed. B. Fraser-Reid, K. Tatsuta, and J. Thiem, Springer Berlin Heidelberg, 2008, pp.3-55.

10. F. O. Talbot and J. P. Simons, Phys. Chem. Chem. Phys. **4**, 3562-3565 (2002).

11. I. Usabiaga, J. González, P. F. Arnáiz, I. León, E. J. Cocinero, and J. A. Fernández, Physical Chemistry Chemical Physics 18, 12457-12465 (2016).

12. J. M. Hollis, F. J. Lovas, A. J. Remijan, P. R. Jewell, V. V. Ilyushin, and I. Kleiner, The Astrophysical Journal. **643**, 25–28 (2006).

13. T. Ebata, Bulletin of the Chemical Society of Japan **82**, 127-151 (2009).

14. E. E. Baquero, W. H. James, S. H. Choi, S. H. Gellman, and T. S. Zwier, Journal of the American Chemical Society **130**, 4784-4794 (2008).

15. I. Compagnon, J. Oomens, G. Meijer, and G. von Helden, Journal of the American Chemical Society **128**, 3592-3597 (2006).

16. E. J. Cocinero, E. C. Stanca-Kaposta, D. P. Gamblin, B. G. Davis, and J. P. Simons, Journal of the American Chemical Society **131**, 1282-1287 (2009).

17. D. Toroz, T. Van Mourik, Molecular Physics **104**, 559-570 (2006).

18. J. Bakker, C. Plutzer, I. Hunig, T. Haber, I. Compagnon, G. von Helden, G. Meijer, and K. Kleinermanns, Chemphyschem **6**, 120-128 (2005).

19. I. Yoon, K. Seo, S. Lee, Y. Lee, and B. Kim, Journal of Physical Chemistry A **111**, 1800-1807 (2007).

20. I. Unamuno, J. A. Fernández, C. Landajo, A. Longarte, and F. Castaño, Chemical Physics **271**, 55-69 (2001).

21. J. A. Fernández, I. Unamuno, A. Longarte, and F. Castaño, Journal of Physical Chemistry A **105**, 961-968 (2001).

22. I . Unamuno, J. A. Fernández, A. Longarte, and F. Castaño, Journal of Physical Chemistry A **104**, 4364-4373 (2000).

23. N. A. Macleod, and J. P. Simons, Physical Chemistry Chemical Physics **6**, 2821-2826 (2004).

24. N. A. Macleod, and J. P. Simons, Physical Chemistry Chemical Physics **5**, 1123-1129 (2003).

25. E. G. Robertson, and J. P. Simons, Physical Chemistry Chemical Physics **3**, 1-18 (2001).

26. I. León, E. J. Cocinero, J. Millán, S. Jaeqx, A. Rijs, A. Lesarri, F. Castaño, and J. A. Fernández, Phys. Chem. Chem. Phys. **14**, 4398 (2012).

27. I. León, J. Millán, E. J. Cocinero, F. Castaño, and J. A. Fernández, ChemPhysChem **13**, 3819-3826 (2012).

28. E. J. Cocinero, P. Carcabal, T. D. Vaden, J. P. Simons, and B. G. Davis, Nature **469**, 76-U1400 (2011).

29. E. J. Cocinero, D. P. Gamblin, B. G. Davis, and J. P. Simons, Journal of the American Chemical Society **131**, 11117-11123 (2009).

30. J. P. Simons, B. G. Davis, E. J. Cocinero, D. P. Gamblin, and E. C. Stanca-Kaposta, Tetrahedron-Asymmetry **20**, 718-722 (2009).

31. Z. Su, E. J. Cocinero, E. C. Stanca-Kaposta, B. G. Davis, and J. P. Simons, Chemical Physics Letters **471**, 17-21 (2009).

32. E. J. Cocinero, E. C. Stanca-Kaposta, M. Dethlefsen, B. Liu, D. P. Gamblin, B. G. Davis, and J. P. 9Simons, Chemistry-A European Journal **15**, 13427-13434 (2009).

33. J. P. Simons, E. C. Stanca-Kaposta, E. J. Cocinero, B. Liu, B. G. Davis, D. P. Gamblin, and R. T. Kroemer, Physica Scripta **78** (2008).

34. I. León, J. Millán, E. J. Cocinero, A. Lesarri, and J. A. Fernández, Angew. Chem. Int. Ed. **52**, 7772-7775 (2013).

35. I. León, J. Millán, E. J. Cocinero, A. Lesarri, and J. A. Fernández, Angew. Chem. Int. Ed. **53**, 12480-12483 (2014)

36. I. León, R. Montero, A. Longarte, and J. A. Fernández, Physical Chemistry Chemical Physics **17**, 2241-2245 (2015).

37. B.J. Gibbons, P.J. Roach, and T. D. Hurley, J. Mol. Biol. **319**, 463–477 (2002).

38. M. Frisch, et al. Gaussian 09, Rev. A02. 2009. Wallingford CT, Gaussian, Inc.

39. S. F. Boys and F. Bernardi, Mol. Phys. **19**, 553-566 (1970).

40. T. Watanabe, T. Ebata, S. Tanabe, and N. Mikami, J. Chem. Phys. **105**, 408-419 (1996).

41. I. León, J. González, J. Millán, F. Castaño, and J. A. Fernández, J. Phys. Chem. A **118**, 2568-2575 (2014).

Figure Captions

Scheme. 1. (a) N-Methylacetamide (mAct); b) β-Phenyl-D-glucopyranoside (β-PhGlc).

Fig. 1. The six most stable conformational isomers of mAct•β-PhGlc calculated at M06-2X/6-311++G(d,p) level, together with their relative stability in kJ/mol. ZPE was applied to all the energy values.

Fig. 2. One-color REMPI spectra of a) mAct·β-PhGlc, b) β-PhGlc and c) phenol.

Fig. 3. IR spectra of mAct•β-PhGlc and the predicted spectra for the structures in Figure 2 calculated at M06-2X/6-311++G(d,p). A correction factor of 0.939 was employed to account for the anharmonicity.

Fig. 4. Gibbs relative free energy of the conformations for mAct·β-PhGlc. The red bar indicates the temperature at which most of the organic compounds decompose, while the blue bar indicates the temperature of decomposition of pyranose. The orange bar indicates where ΔG becomes positive and therefore, the cluster is no longer stable.

Fig. 5. IR spectra of mAct•β-PhGlc and the predicted spectra for the structures in Figures 2 and 3, together with the detected species. Two different families are detected: isomers 2, 3 and 6 only differ in a small displacement in the relative position of both molecules, while conformer 2 isomerizes into conformer 1 through the rotation of the hydroxymethyl group. Conformer 4 is also detected and corresponds to another family due to the different points of interaction. Conformer 5, on the other hand, is not detected experimentally.

Scheme 1

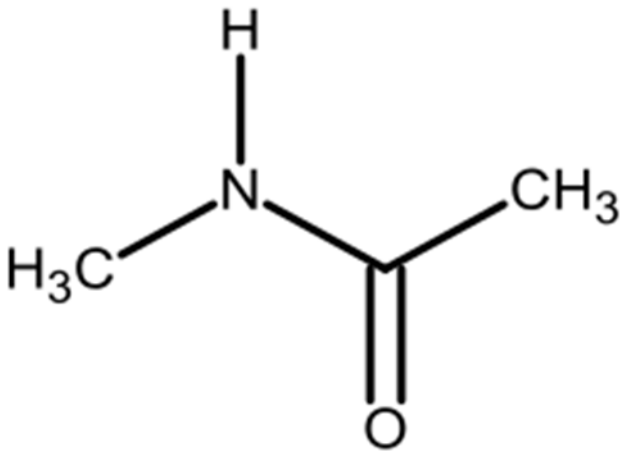

N-methylacetamide

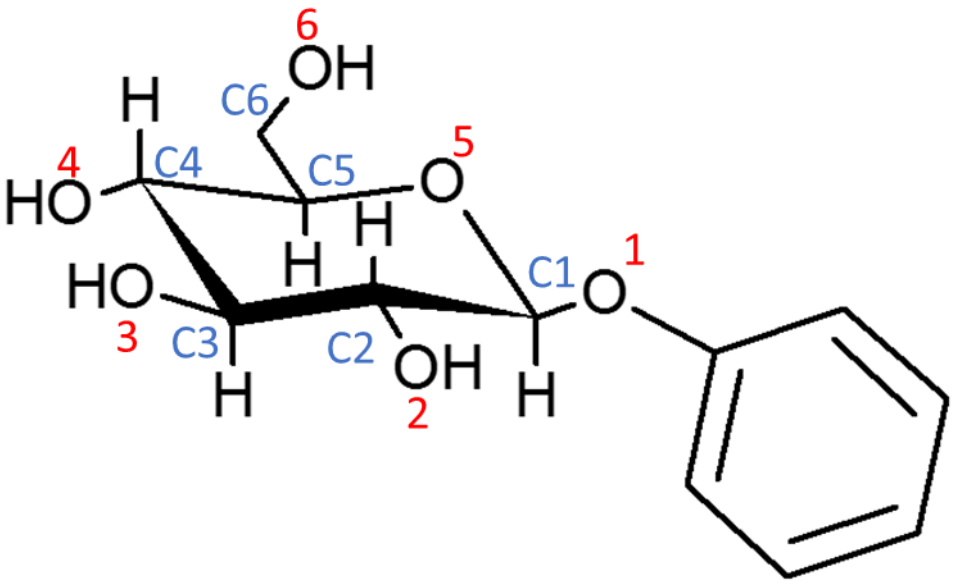

β-Phenyl-D-glucopyranoside

Fig. 1

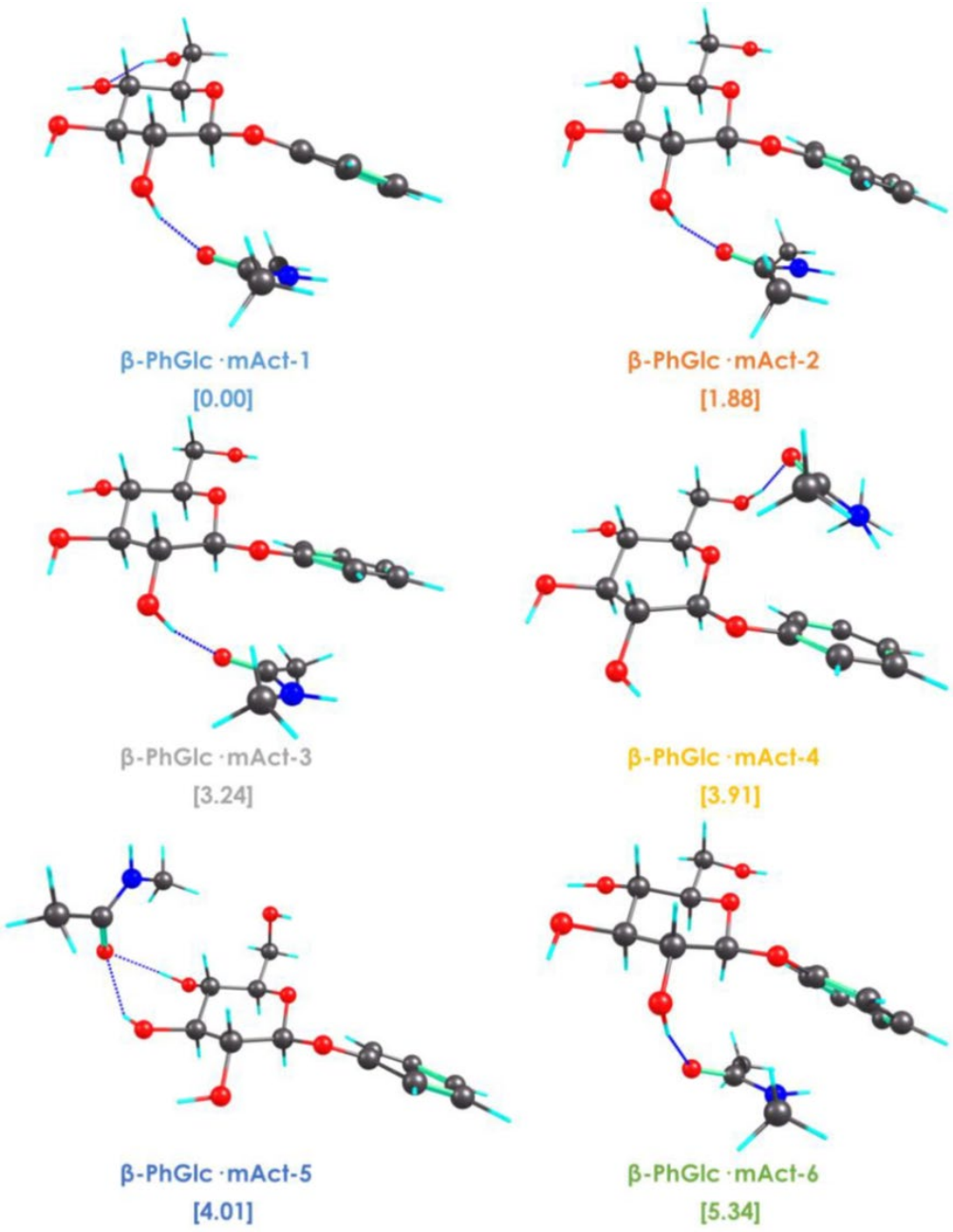
β-PhGlc ·mAct-1
[0.00]
β-PhGlc ·mAct-2
[1.88]
β-PhGlc ·mAct-3
[3.24]
β-PhGlc ·mAct-4
[3.91]
β-PhGlc ·mAct-5
[4.01]
β-PhGlc ·mAct-6
[5.34]

Fig. 2

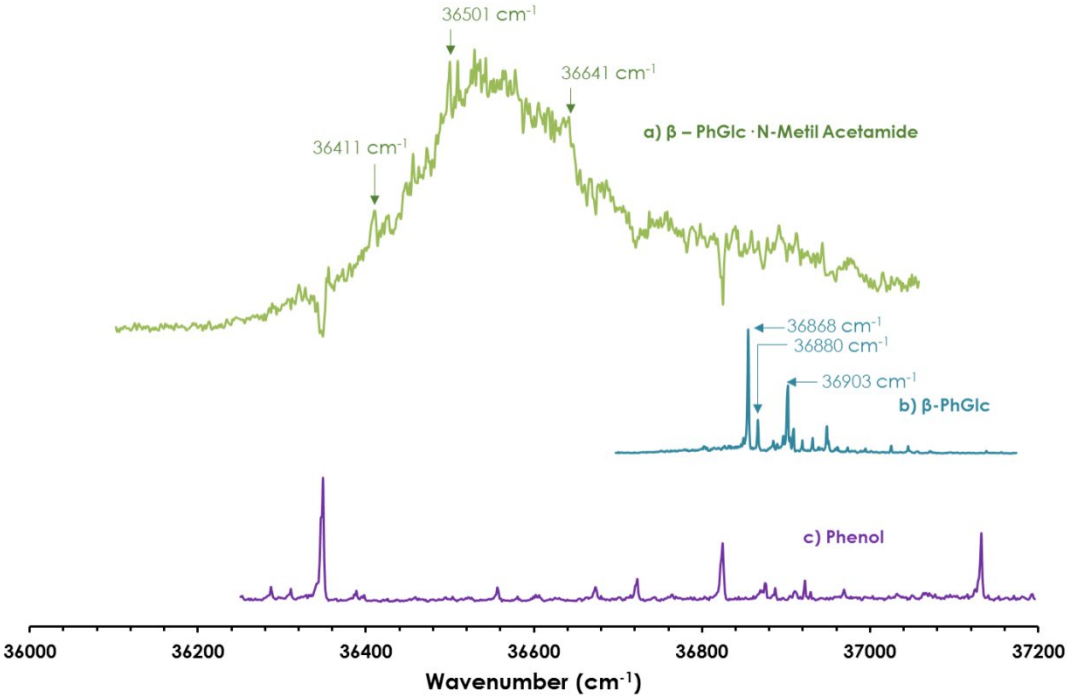
36501 cm-1
36641 cm-1
36411 cm-1
a) β – PhGlc ·N-Metil Acetamide
36868 cm-1
36880 cm-1
36903 cm-1
b) β-PhGlc
c) Phenol
36000
36200
36400
36600
36800
37000
37200
Wavenumber (cm-1)

Fig. 3

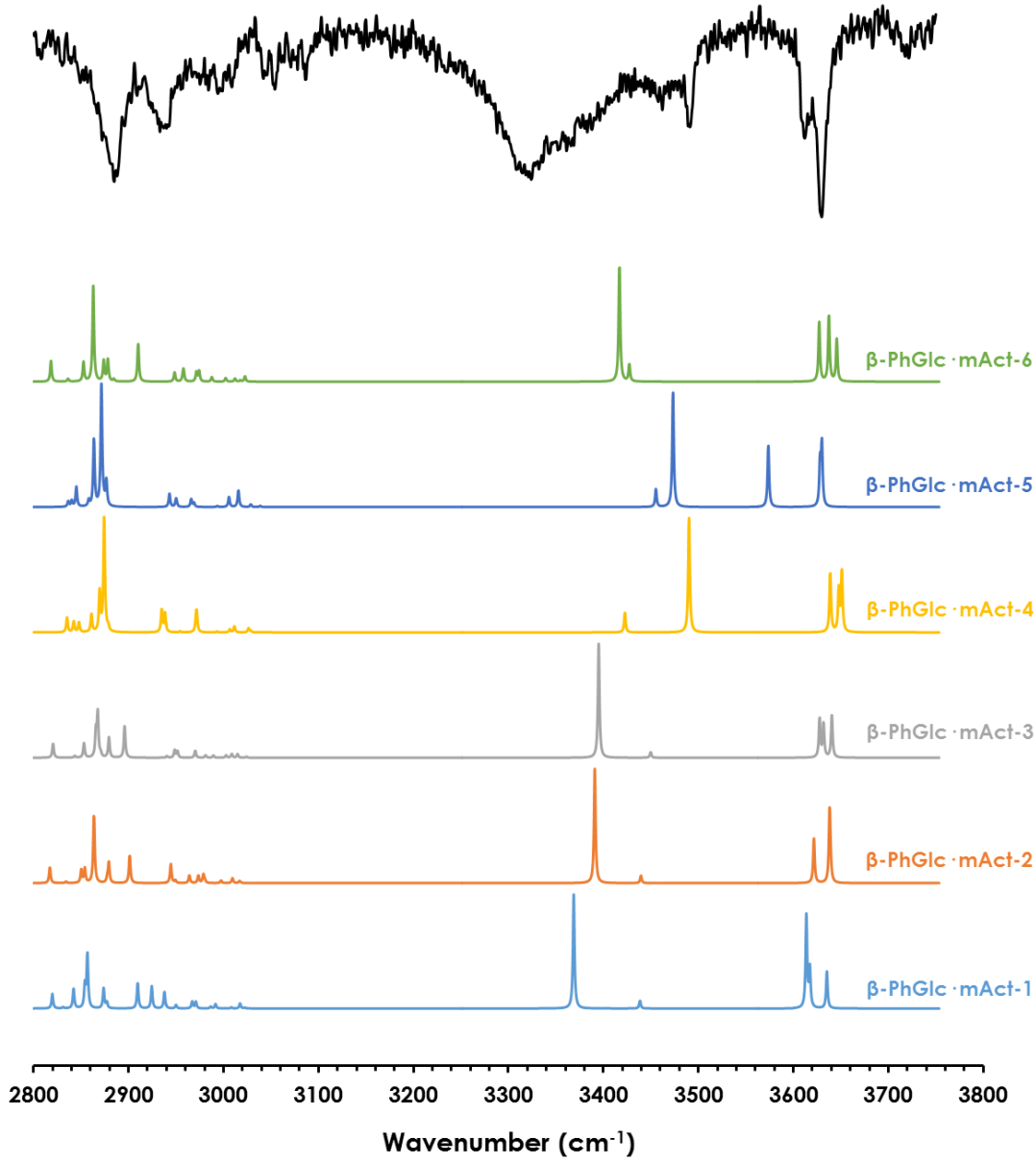
β-PhGlc·mAct-6
β-PhGlc·mAct-5
β-PhGlc·mAct-4
β-PhGlc·mAct-3
β-PhGlc·mAct-2
β-PhGlc·mAct-1
2800
2900
3000
3100
3200
3300
3400
3500
3600
3700
3800
Wavenumber (cm-1)

Fig. 4

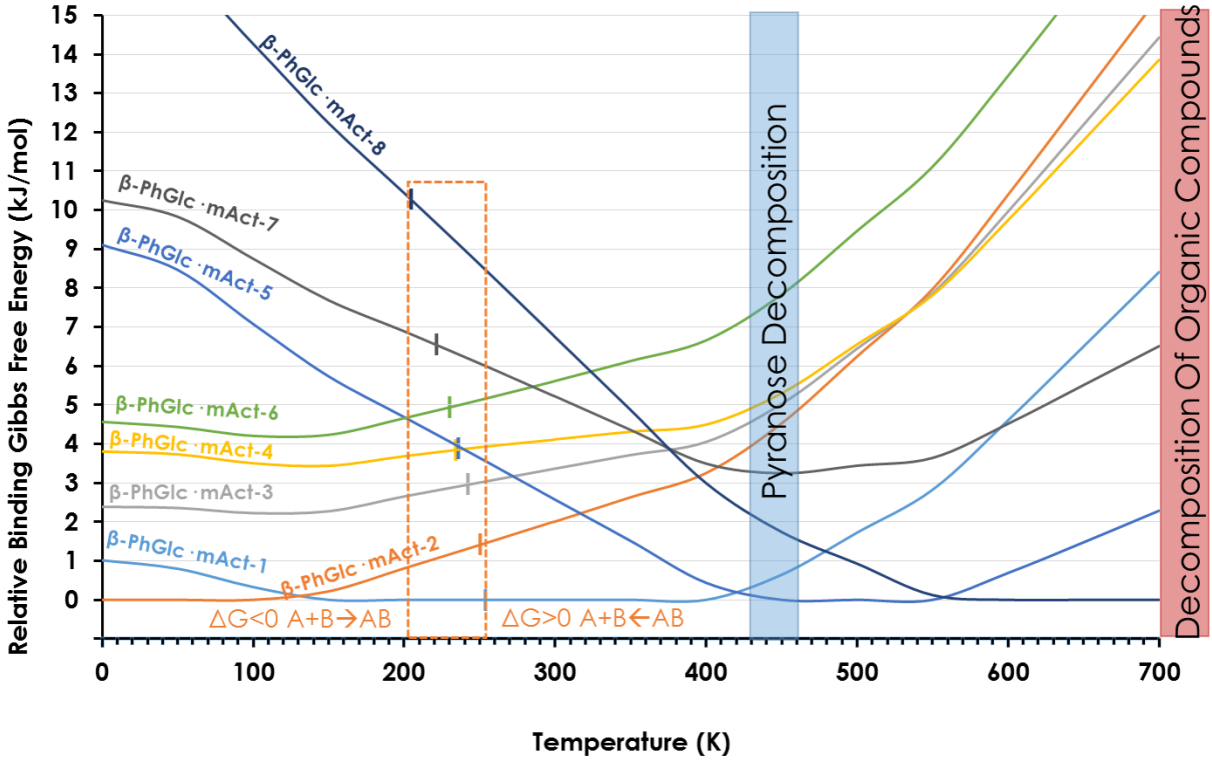
Relative Binding Gibbs Free Energy (kJ/mol)
Temperature (K)
β-PhGlc ·mAct-8
β-PhGlc ·mAct-7
β-PhGlc ·mAct-5
β-PhGlc ·mAct-6
β-PhGlc ·mAct-4
β-PhGlc ·mAct-3
β-PhGlc ·mAct-1
β-PhGlc ·mAct-2
ΔG<0 A+B→AB
ΔG>0 A+B←AB
Pyranose Decomposition
Decomposition Of Organic Compounds

Fig. 5

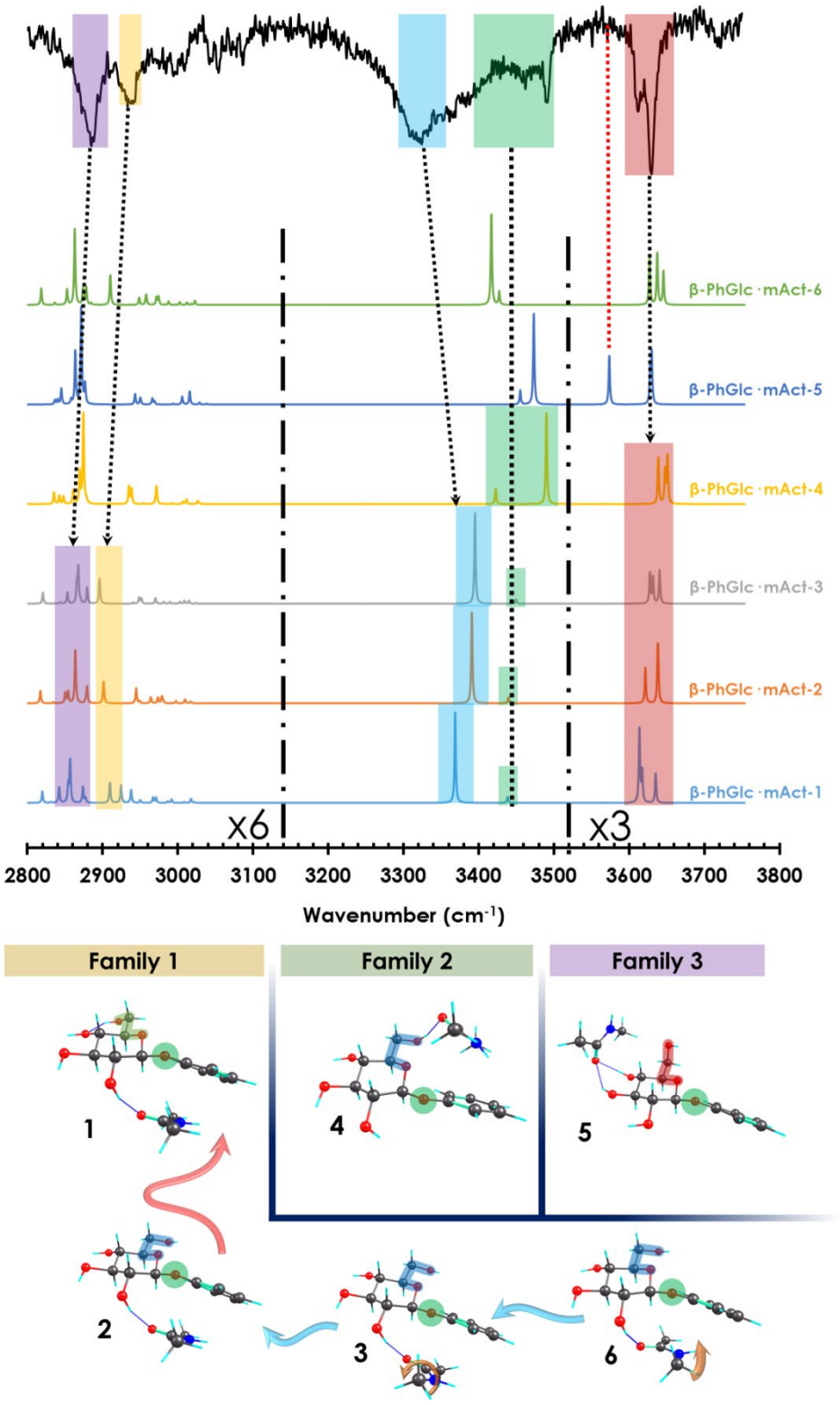
β-PhGlc·mAct-6
β-PhGlc·mAct-5
β-PhGlc·mAct-4
β-PhGlc·mAct-3
β-PhGlc·mAct-2
β-PhGlc·mAct-1
x6
x3
2800
2900
3000
3100
3200
3300
3400
3500
3600
3700
3800
Wavenumber (cm-1)
Family 1
Family 2
Family 3
1
2
3
4
5
6